ResearchGate

See discussions, stats, and author profiles for this publication at: https://www.researchgate.net/publication/233872582

Influence of the O-protonation in the OC-O-Me Z preference. A QTAIM study

ARTICLE *in* THE JOURNAL OF PHYSICAL CHEMISTRY A · DECEMBER 2012

Impact Factor: 2.69 · DOI: 10.1021/jp311472b · Source: PubMed

CITATIONS
4

READS
24

2 AUTHORS:

David Ferro-Costas
University of Vigo
13 PUBLICATIONS **33** CITATIONS
SEE PROFILE

Ricardo Mosquera
University of Vigo
144 PUBLICATIONS **1,814** CITATIONS
SEE PROFILE

Available from: David Ferro-Costas
Retrieved on: 26 January 2016

THE JOURNAL OF PHYSICAL CHEMISTRY A

Article

pubs.acs.org/JPCA

Influence of the O-Protonation in the O═C−O-Me *Z* Preference. A QTAIM Study

David Ferro-Costas and Ricardo A. Mosquera*

Departamento de Química Física, Facultade de Química, Universidade de Vigo, Lagoas-Marcosende s/n, 36310 Vigo, Galicia, Spain

ABSTRACT: One of the three O-protonations of methyl formate (MF) gives rise to a system where the *Z* preference is switched off and the *E* conformer becomes the most stable arrangement. The quantum theory of atoms in molecules scheme for splitting the physical space of a molecule into atomic subspaces has been employed to analyze this trend, as well as the effect of the protonation in MF. The most important changes in energy and electron density upon protonation do not take place when MF reorganizes its nuclei, but when the proton is introduced explicitly. The same trend is observed when the H attached to the carbonyl C is replaced by electron donating and withdrawing groups (CN, F, OH, CH_3, and CF_3). The origin of the inversion in the conformational preference relies in the changes experienced by two interactions: (i) the methyl group with the proton and (ii) that between the atoms of the ether C−O bond.

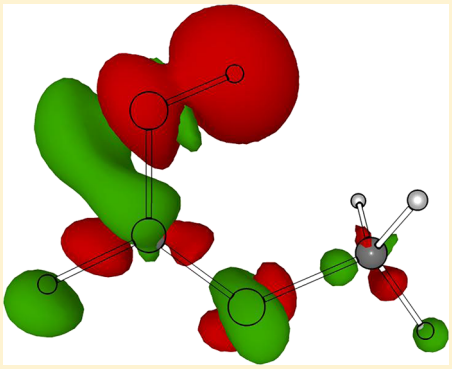

1. INTRODUCTION

The *Z* effect is a conformational preference exhibited by esters, secondary amides, and related molecules containing R′COOR or similar units (R and R′ denoting H or alkyl groups) where, in general, the *Z* conformer is more stable than the *E* one (Figure 1).[1] The importance of obtaining a clear understanding of this effect arises from the fact that around 99.95% of the peptide bonds established in proteins between amino acid residues (excepting proline) display *Z* arrangement.[2]

The most common explanation used in the chemical literature for this preference (as well as for the anomeric effect, which has been considered similar, at least in part) is based on the hyperconjugative model (HM).[1] According to this model, the *Z* stabilization is associated with a hypothetical delocalization of the electron lone pair (*lp*) of the ether oxygen over the σ antibonding molecular orbital of the C═O bond (*in-plane* interaction). However, recent studies based on valence bond theory[3] have provided strong evidence that hyperconjugative interactions are not responsible for the anomeric effect. Indeed, even the quantum theory of atoms in molecules (QTAIM)[4,5] analysis of the electron density (ρ) reorganizations accompanying the *E* to *Z* interconversion shows some incompatibilities with this HM interpretation.[6] Thus, in formic acid (the simplest system exhibiting *Z* preference), the ether oxygen increases its electron density population when the *E* conformer interconverts into the *Z* one,[6] while the HM predicts the reverse electron density displacement.

Besides, the QTAIM disjoint partitioning of the real space into atoms allows us to split the electronic molecular energy into monatomic and diatomic contributions directly derived from the molecular Coulomb Hamiltonian. Looking at the results of this partitioning in formic acid,[6] we have found that the core attraction interaction between the electron density of the carbonyl oxygen and the acid hydrogen nucleus is the most important energy term that favors *Z* preference. Results obtained through this QTAIM-based energy partitioning in other molecules (methyl formate, acetic acid, and *N*-methyl formamide), also indicate that the *Z*-preference displayed in diverse X═C−Y−R units (X = O and Y = O, N) is basically favored by the interaction of the X···R pair. It has to be remarked that this interaction also makes possible to explain the *Z* effect in secondary amides, which cannot be justified within the framework of the HM due to the lack of one nitrogen *lp* in the O═C−N plane.

We want to highlight that getting insight on the physical origin of inversions of conformational trends is of interest for proposing new synthesis routes of molecules where non-conventional arrangements become the preferred ones. Thus, the formation of intramolecular hydrogen bonds explains why attaching certain groups in a polysubstituted cyclohexane (for example, α = β = γ = OH in Scheme 1) reverses the conformational preference for equatorial arrangements. This reversion can be a first step in the synthetic route for a polycyclic system (Scheme 1). In this vein, the modification of the central X═C−Y structure may affect the *Z*-conformational preference in diverse ways. Alkylation and/or O/S replacement have been already studied.[6] This paper aims to analyze the effect of the O-protonations of the O═C−O−Me moiety (Figure 2), which can be of practical interest as one of them reverses the *Z*-preference.

2. COMPUTATIONAL DETAILS

Z and *E* conformers of methyl formate (MF) and of its O-protonations (a total of 8 structures) were optimized and

Received: November 20, 2012
Revised: December 5, 2012
Published: December 5, 2012

ACS Publications © 2012 American Chemical Society

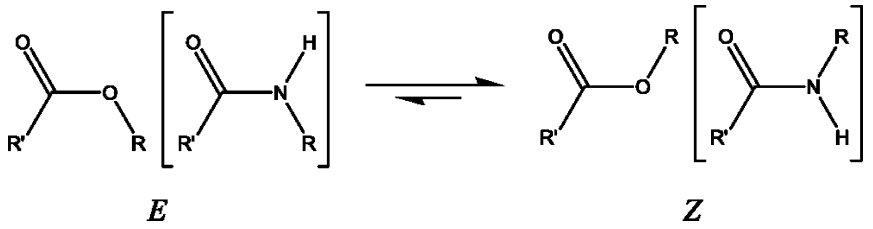

Figure 1. *Z*/*E* conformers for R′COOR molecules. Both conformers are shown in brackets for secondary amides.

Scheme 1

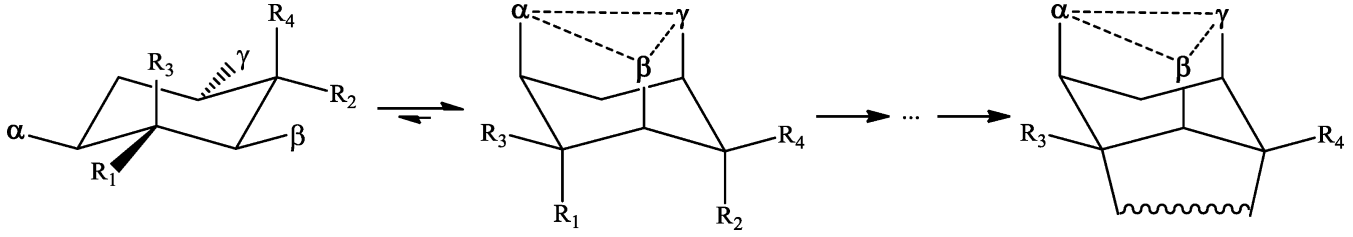

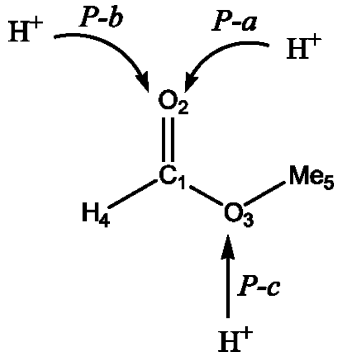

Figure 2. Nomenclature of the O-protonations in methyl formate and atom/group labels.

characterized as minima in the frequencies calculation at the HF, B3LYP, and MP2 levels using the Gaussian 03 program[7] with the standard 6-311++G(2d,2p) 6d basis set. CCSD optimizations were also effectuated for the cases where the QTAIM-based energy partitioning was performed (see below). In the case of MF, its HF-optimized geometry (for the ***E*** conformer) is not coincident with those obtained at the remaining computational levels, whose main difference is centered in the internal rotation of the methyl group.[6] Moreover, the ***Z*** and ***E*** conformers of five MF derivatives (R′ = F, OH, CN, CF_3, and CH_3, being R′ the group attached to carbonyl C), and their corresponding protonated forms that reverse the ***Z***-preference, were also studied at the B3LYP/6-311++G(2d,2p) 6d level.

The QTAIM topological electron density analysis was carried out with the AIMPAC package of programs,[8] which obtains atomic basins (Ω) and their corresponding properties, such as electron population, $N(\Omega)$, and energy, $E(\Omega)$. Integration errors, expressed as differences between total properties and those obtained by summation of those of the fragments [$N - \Sigma N(\Omega)$ and $E - \Sigma E(\Omega)$], were always smaller (in absolute value) than 1.2×10^{-3} au and 0.5 kJ mol^{-1}, respectively. The absolute values achieved for $L(\Omega)$ were always smaller than 9×10^{-4} au.

QTAIM-based molecular energy partitioning was performed (for ***Z*** and ***E*** conformers of MF and of one of its protonations), as previously shown,[6] splitting the total CCSD molecular energy, E_{CCSD}, into (eq 1): *(i)* correlation energy, E_{corr}^{CCSD}, defined as the difference between E_{CCSD} and the Hartree−Fock energy (E_{HF}) of the system, *(ii)* atomic electron kinetic energies $K(\Omega)$, *(iii)* core-attraction interaction energies of the nucleus Z by the Ω-electron density, $V_{ne}(Z,\Omega)$, *(iv)* classical Coulomb electron−electron repulsion energies (defined with self-interaction) between basins Ω and Ω', $V_{EE}(\Omega,\Omega')$, *(v)* electron−electron exchange interactions $V_X(\Omega,\Omega')$, and *(vi)* Coulomb repulsions between nuclei Z and Z′, $V_{nn}(Z,Z')$.

$$E_{HF} = E_{CCSD} - E_{corr}^{CCSD} = \sum_{\Omega}[K(\Omega) + \sum_{Z} V_{ne}(Z,\Omega)] + \sum_{\Omega' \geq \Omega} \sum [V_{EE}(\Omega,\Omega') + V_X(\Omega,\Omega')] + \sum_{Z' > Z} \sum V_{nn}(Z,Z') \quad (1)$$

Terms from *ii* to *iv* were obtained using the HF electron density obtained for the CCSD-optimized geometries, performing single and double integrations over the atomic basins and pairs of basins through the STOCK program.[9]

Collecting all of the two-atom contributions, a total interatomic interaction energy between QTAIM-atoms A and B, $V_T(A,B)$, can be defined as:

$$V_T(A,B) = V_{ne}(Z_A,\Omega_B) + V_{ne}(Z_B,\Omega_A) + V_{EE}(\Omega_A,\Omega_B) + V_X(\Omega_A,\Omega_B) \quad (2)$$

In such manner, eq 1 can be rewritten as:

$$E_{CCSD} - E_{corr}^{CCSD} = \sum_{\Omega} E_{net}(\Omega) + \frac{1}{2} \sum_{A \neq B} \sum V_T(A,B) \quad (3)$$

where the atomic net energy of a given atom has been defined as:

$$E_{net}(\Omega_A) = K(\Omega_A) + V_{ne}(Z_A,\Omega_A) + V_{EE}(\Omega_A,\Omega_A) + V_X(\Omega_A,\Omega_A) \quad (4)$$

dx.doi.org/10.1021/jp311472b | J. Phys. Chem. A 2013, 117, 257−265

When a chemical group has to be considered, the interaction energy between the functional group G and an atom B is given by:

$$V_T(G, B) = \sum_{A \in G} V_T(A, B) \tag{5}$$

where B$\notin G$. On the other side, the net energy of a group can be defined by adding the net energies of its constituents and their total intragroup interaction energies, that is:

$$E_{net}(G) = \sum_{A \in G} E_{net}(A) + \frac{1}{2} \sum_{A \in G} \sum_{\substack{B \in G \\ B \neq A}} V_T(A, B) \tag{5a}$$

Generalizing, the QTAIM provides us with a way for splitting the total HF energy of a system into the sum of the net energies for each subsystem and the pair-interactions among them:

$$E_{CCSD} - E_{corr}^{CCSD} = \sum_{S} E_{net}(S) + \frac{1}{2} \sum_{S \neq S'} \sum V_T(S, S') \tag{6}$$

Here S and S′ are subsystems of the total system (atoms or group of atoms as, for example, functional groups).

It is important to highlight that eq 6 is the chief equation in this partition scheme, in similarity with the one proposed by Blanco et al.[10]

3. RESULTS AND DISCUSSION

The three different O-protonations of MF (Figure 2) have been studied. In protonation *P-a*, the proton (in what follows, H_p) is bonded to the carbonyl oxygen and directed toward ether-O; in *P-b*, the proton at carbonyl-O is placed at the opposite side; and, finally, in *P-c*, the proton is bonded to ether-O.

The results provided with the different computational levels correlate quite well (especially those that take into account the correlation energy, as it can be seen in Figure 3). Consequently, we only analyze the MP2 results in this paper, with the exclusion of the data from the QTAIM-based energy partitioning (see previous section), and those associated with the MF derivatives. Taking into account the computational cost involved for the latter and the good correlation among levels, MF derivatives were only studied at the B3LYP level.

The most stable of the six possible protonated forms for MF is the result of *P-b* over the ***Z*** conformer (Table 1). In contrast, *P-c* protonations give rise to the least stable ones, where the O═C−O−C moiety is not planar (the dihedral angle is 13.3° for ***Z*** and 148.5° for ***E***, at the MP2 level) and the C1−O3 bond lengthens significantly with regard to unprotonated MF (Table 1).

The electron density reorganizations accompanying the protonations give rise to changes in atomic electron populations and energies (Figure 4 and Table 2). In all of them, the final ρ gained by the proton is between 0.310 and 0.325 au. Therefore, as pointed out in previous papers on the protonations of oxygen and nitrogen containing compounds, and contrasting with traditional Lewis structures, the molecular electron density distribution of the protonated form is more compatible with a positive charge on the proton than on any heteroatom.[11−15]

Moreover, although the resonance model (RM) predicts (Figure 5) that the electron population over the carbonyl oxygen should be lower at *P-a* and *P-b* protonated forms, its population increases (or remains almost constant) in both ***E*** forms and in the ***Z*** one of *P-b* (Figure 4) with regard to the corresponding unprotonated conformer. Therefore, not only the HM, but also the RM's predictions display inconsistencies with the QTAIM results, as it was also previously observed.[16−18]

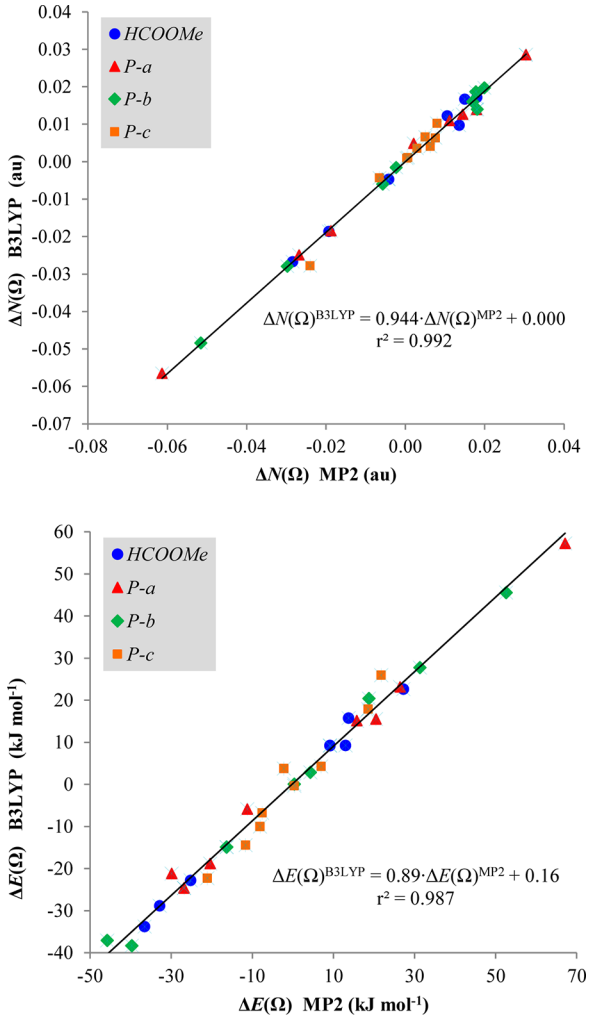

Figure 3. Plot of the $\Delta N(\Omega)$ and $\Delta E(\Omega)$ values (in au and kJ mol^{-1}, respectively) obtained at MP2 and B3LYP levels.

We observe that *P-a* and *P-b* protonations have similar effects on electron density reorganization (Figure 4). In them, the total population $N(\Omega)$ of the two oxygens (especially that of the protonated one) is nearly unaffected (Figure 4) and, as in previous QTAIM studies,[13,15] most of the electron population gained by H_p is not taken from the protonated atom but from the rest of the molecule, particularly from the hydrogens (H4 and methyl hydrogens), which lose from 0.364 to 0.400 au. It is important to note that in all protonations (even in *P-c*), the methyl carbon always increases its electron population (between 0.112 and 0.133 au) respect to the neutral molecule, so the whole density that comes out of the methyl group is provided by its hydrogens.

Otherwise, the ρ redistribution yielded by *P-c* protonations is significantly different. We observe an important variation in the population of both the oxygens, particularly the unprotonated one (it loses around double electron density than the other). In fact, the total variation of electron density in both oxygens accounts for 62 to 67% of the electron density received by H_p. Nonetheless, this does not mean this electron density reaches H_p because the carbonyl carbon increases its electron

dx.doi.org/10.1021/jp311472b | J. Phys. Chem. A 2013, 117, 257−265

Table 1. Energy of the *Z* Conformer (E_Z, in au) and Energy Difference between *Z* and *E* Conformers ($\Delta_{ZE}E$, in kJ mol^{-1}) for Methyl Formate and Its O-Protonations Here Studied[a]

	E_Z				$\Delta_{ZE}E = E_Z - E_E$				d_{C1-O3} (Å)	
molecule	HF	B3LYP	MP2	CCSD	HF	B3LYP	MP2	CCSD	*Z*	*E*
HCOOMe	−227.867 08	−229.148 68	−228.601 17	−228.616 68	−23.5	−19.8	−23.1	−22.9	1.343	1.350
P-a	−228.179 75	−229.451 53	−228.900 12	−228.921 97	17.8	16.3	14.4	14.6	1.262	1.260
P-b	−228.186 68	−229.458 20	−228.906 91		−10.4	−9.0	−11.1		1.253	1.254
P-c	−228.145 52	−229.423 14	−228.876 42		−3.2	−2.3	−3.4		1.579	1.578

[a]The bond length (*d*, in Å) for the C1−O3 bond, obtained at the MP2 level, is also shown.

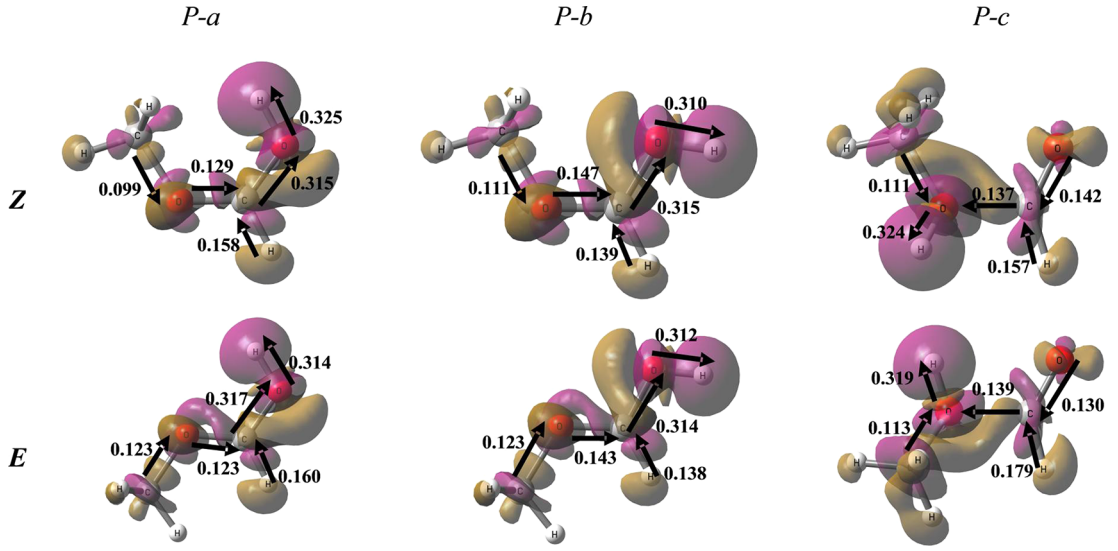

Figure 4. Electron density reorganizations due to the diverse protonations (MP2). Black arrows and numbers (in au) indicate interatomic transferences of electron density upon protonation, obtained considering the optimized protonated and unprotonated molecules. The $\Delta\rho$ isosurfaces of ±0.005 au are also shown (the reference density is that of the parent molecule in the geometry of the protonated form). Positive isosurface is in lilac while the negative one is in brown.

Table 2. Relative MP2 QTAIM Atomic Energies (in kJ mol^{-1}) for the Three O-Protonations with Regard to the Initial Molecule[a]

	Z			*E*		
Ω	$E_{P\text{-}a}(\Omega) - E_{MF}(\Omega)$	$E_{P\text{-}b}(\Omega) - E_{MF}(\Omega)$	$E_{P\text{-}c}(\Omega) - E_{MF}(\Omega)$	$E_{P\text{-}a}(\Omega) - E_{MF}(\Omega)$	$E_{P\text{-}b}(\Omega) - E_{MF}(\Omega)$	$E_{P\text{-}c}(\Omega) - E_{MF}(\Omega)$
C1	97.0	104.6	−256.8	94.1	117.6	−287.4
O2	−140.0	−142.4	−168.0	−146.8	−129.1	−146.1
O3	−203.5	−213.6	228.2	−244.5	−257.6	184.4
H4	173.7	154.7	194.8	174.5	150.6	215.1
Me5	92.8	76.3	84.8	85.3	90.8	86.0
H_p	−804.7	−782.5	−805.6	−784.3	−786.8	−794.0

[a]$E_{MF}(\Omega)$ represents the energy of the basin Ω in MF.

population (around 0.17 au), which is not observed in any other protonation.

In conclusion, the introduction of a proton in the system produces a flux of ρ from the whole molecule to H_p. The reorganization of ρ in protonations *P-a* and *P-b*, which mainly affects the population of hydrogens, behaves according to what was observed for other protonations on electronegative heteroatoms in previous papers. Nevertheless, this changes in *P-c*, where a non-negligible variation in the population of heteroatoms is observed.

3.1. The Protonation Process: From Methyl Formate to Its *P-a* Protonation. In order to analyze the protonation process we have distinguished between (Figure 6): *(i)* geometry deformation, where the molecule reorganizes the position of its nuclei in order to accept the proton (the final geometry, MF_*P-a*, is the one of the HCOOMe moiety in the *P-a* optimized structure), and *(ii)* the insertion of the proton in the new nuclear arrangement (isosurfaces of $\Delta\rho$ are shown in Figure 4). The total electron population reorganization accompanying the first step looks irrelevant in comparison with the one that arises in the second step (Figure 6). Thus, the

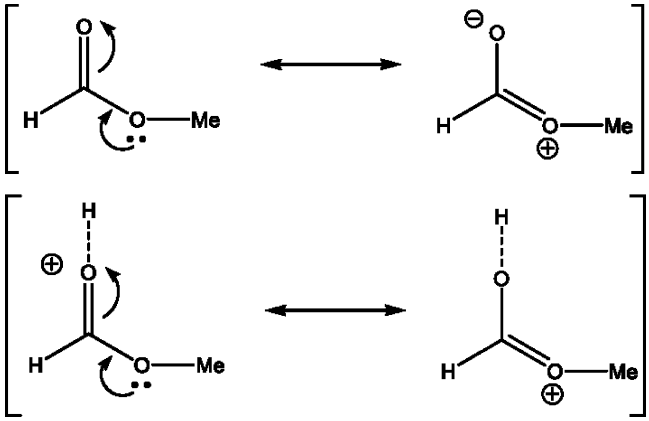

Figure 5. Resonance forms, valid for *Z* and *E* conformers, of HCOOMe and of its *P-a* and *P-b* protonations. The two dots over the ether oxygen represent its two π electrons.

dx.doi.org/10.1021/jp311472b | J. Phys. Chem. A 2013, 117, 257−265

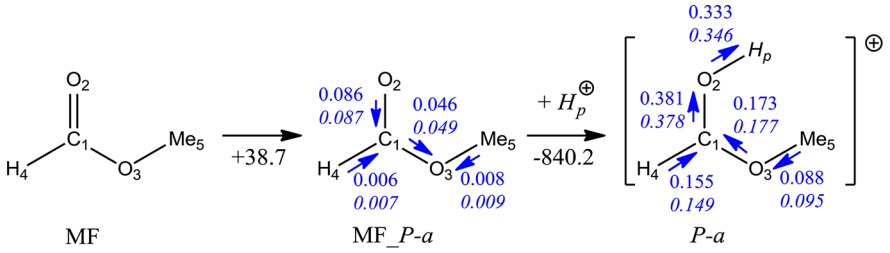

Figure 6. Two steps considered in the *P-a* protonation process (in gas phase) of *Z*-MF. The numbers under the arrows that go from one system to the other represent the variation of the CCSD energy (in kJ mol^{-1}). The variation in the total electron population for each process is also shown, in au, for CCSD and B3LYP levels (the latter in *italics*).

Table 3. Variation in Interaction Energies, Net Energies, and Correlation Energy in the Two Steps of the *P-a* Protonation of *Z*-HCOOMe (Values in kJ mol^{-1})

	MF → MF_*P-a* ΔE_{corr} = −4.2					
$\Delta V_T(A,B)$	C1	O2	O3	H4	Me5	$\Delta E_{net}(B)$
C1						−104.4
O2	658.3					−316.8
O3	−423.2	−36.0				157.2
H4	7.5	−0.8	−9.2			4.3
Me5	−30.4	66.1	117.7	0.2		−48.8
	MF_*P-a* → *P-a* ΔE_{corr} = 24.1					
$\Delta V_T(A,B)$	C1	O2	O3	H4	Me5	H_p	$\Delta E_{net}(B)$
C1							30.6
O2	14.9						257.3
O3	−62.3	24.8					−37.3
H4	289.6	−133.6	−146.6				52.6
Me5	32.8	−33.8	57.6	60.3			31.6
H_p	1118.3	−1640.5	−564.8	89.0	288.9		−593.6

most important change in the population of each atom/group takes place upon the explicit introduction of the proton in the system.

Both steps were analyzed in the case of the *P-a* protonation of the *Z* conformer of MF, carrying out the QTAIM-based energy partitioning (see Computational Details). Taking into consideration only the HCOOMe structure, the effect of the nuclei reorganization is, generally, more significant than the effect of the H_p-introduction when the individual terms are considered (more important changes in E_{net} and V_T for each subsystem or pair of subsystems in the first step, Table 3). However, the variation in E_{net} for this moiety (HCOOMe) is 41.7 kJ mol^{-1} for the MF → MF_*P-a* step (which is the ΔE_{HF} for the CCSD optimized geometries), albeit the variation in the second step (MF_*P-a* → *P-a*) is around 10 times bigger (438.6 kJ mol^{-1}). In any manner, the effect of the protonation, either in the nuclei-reorganization as well as in the introduction of the proton, implies a destabilization of the HCOOMe moiety. Nevertheless, the flux of electron density, that takes place in the second step (Figure 4) to surround H_p with a negative charge distribution, allows H_p to reach around 45% of the energy of the H atom (E_{net} for H_p is −0.22610 au), although $N(H_p)$ is only 0.333 au (0.285 au with HF electron density on CCSD optimized geometry). Moreover, the interaction of H_p with the HCOOMe fragment accounts for −709.1 kJ mol^{-1}. In such manner, the stabilizing part of this process comes from the interaction of the H_p with the HCOOMe moiety and from the stabilization that takes place in H_p due to the introduction of electron population in its QTAIM-basin, not from the modification of the HCOOMe fragment.

3.2. *P-a* Protonation Process in Methyl Formate Derivatives. In order to assess the effects of electron donating and withdrawing R′ groups in the protonation process, we have considered different MF derivatives, where R′ = H has been replaced. Specifically, CF_3 was selected as an example of σ-acceptor, CN as σ and π-acceptor, F as σ-acceptor and weak π-donor, CH_3 as σ-donor, and OH as π-donor and σ-acceptor.

Figure 7 summarizes the electron density transferences that take place in the two steps considered in the previous section for parent MF. In all cases, the inclusion of the proton was again the step with the most significant electron density reorganization. The ρ-reorganization affecting the H_p−O═C−O−CH_3 moiety is basically the same along the series of molecules (Figures 6 and 7), while the donor/acceptor effect of the group only gives rise to significant modifications in the R′-C electron density transference. In fact, the transference for the total process from R′ to carbonyl C varies from 0.047 au in R′ = F to 0.261 au in R′ = CN (Figure 7). We also observe that, as previously reported in benzene[19] and heterocycle derivatives,[20,21] the σ-acceptor character exceeds the π-donor one in OH and F, as these groups lose less electron density than H upon *P-a* protonation. In contrast, CN and CF_3 groups, considered as good ρ-acceptors, lose more electron density than H and CH_3 upon protonation, displaying the largest transference from R′ to the carbonyl C.

3.3. The Effect of the *P-a* Protonation in the *Z/E* Electron Reorganization. It is noteworthy that the introduction of the proton induces an important movement of the electron density toward the positive charge, bigger than the one that takes place in the deformation of the molecule

dx.doi.org/10.1021/jp311472b | J. Phys. Chem. A 2013, 117, 257−265

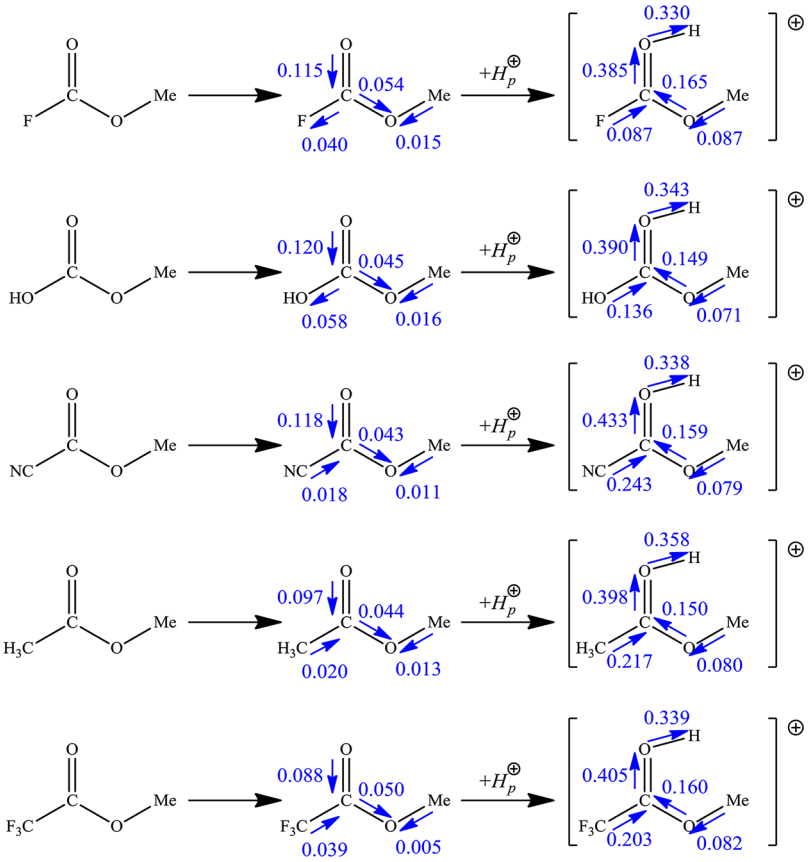

Figure 7. Two steps considered in the *P-a* protonation process (in gas phase) of diverse **Z**-MF derivatives. The variation in the total electron population (computed from B3LYP electron densities) for each process is shown (in au).

Table 4. $\Delta_{ZE}N$ and $\Delta_{ZE}E$ Values (the First One in au Multiplied by 10^3 and the Second One in kJ mol^{-1}) for HCOOMe and for the Three O-Protonations at the MP2 Level[a]

	HCOOMe		*P-a*		*P-b*		*P-c*	
	$\Delta_{ZE}N$	$\Delta_{ZE}E$	$\Delta_{ZE}N$	$\Delta_{ZE}E$	$\Delta_{ZE}N$	$\Delta_{ZE}E$	$\Delta_{ZE}N$	$\Delta_{ZE}E$
C1	13.6	−32.8	18.0	−29.9	18.1	−45.8	6.3	−2.2
O2	15.0	13.7	2.1	20.5	17.8	0.3	2.9	−8.1
O3	10.5	−25.3	−18.8	15.7	−5.7	18.8	0.7	18.6
H4	−28.4	27.2	−26.8	26.4	−29.7	31.3	−6.5	6.9
Me5	−9.7	−5.4	13.9	2.1	2.4	−19.9	−8.0	−6.6
H_p			11.1	−20.4	−2.3	4.3	5.0	−11.7

[a]All these values have been obtained by subtraction of ***E*** values from ***Z*** ones.

(MF → MF_*P-a*). In such a way, the proton can be considered to play the leading role in the electron reorganization (MF_*P-a* → *P-a*). As a result of the size of that electron density rearrangement, and the presence of the partial positive charge allocated in H_p (+0.667 au) it is likely to expect that any electron density restructuring, as the one arising from the ***Z***/***E*** interconversion, is going to be different from that of the neutral molecule. Taking heed of this important point, we analyze the reorganization of electron density involved in the ***Z***/***E*** change of the different protonated forms.

It is of importance to highlight that the ***E*** form is, and not the ***Z*** one, the most stable in *P-a* (Table 1) and, for this reason, this protonation has more relevance for us than the others, as it reverses the ***Z*** effect.

Z/***E*** electron density reorganization shown by *P-a* protonated form (Table 4) is clearly different to that of the parent molecule (HCOOMe). Also, the evolution of the bond distances follows different trends. Thus, for example, Δd_{C1-O3} and $\Delta d_{O3\text{-}Me}$ are −0.007 and +0.008 Å for MF and +0.002 and −0.008 Å for this protonation, at the MP2 level.

The most outstanding difference appears in $\Delta_{ZE}N$(Me5) values ($\Delta_{ZE}N = N_Z - N_E$) and, as Me5 is attached to O3, in $\Delta_{ZE}N$(O3). In the protonated form, $\Delta_{ZE}N$(Me5) is positive, whereas it is negative for HCOOMe. A possible qualitative explanation can be based on the directionality of the electron density transfer[15] with respect to the positive charge associated with H_p (see Appendix), as we could anticipate from the discussion at the beginning of this subsection.

With regard to the inversion of the ***Z*** preference (Table 1), QTAIM-based energy partitioning has been performed (using HF electron densities and basins for the CCSD ***Z*** and ***E*** optimized geometries) for HCOOMe and *P-a*. Table 5 lists the differences between them. First we observe that differences due to correlation energy, $\Delta\Delta_{ZE}E_{corr}$, are negligible. As it is obvious,

dx.doi.org/10.1021/jp311472b | J. Phys. Chem. A 2013, 117, 257−265

Table 5. Difference in the *E* to *Z* Variation of the Net, Interaction, and Correlation Energies between *P-a* and MF (and also MF_*P-a* with Regard to MF and *P-a* with Regard to MF_*P-a*)[a]

	$\Delta_{Z\text{-}E}$(MF_*P-a*) − $\Delta_{Z\text{-}E}$(MF) (1)							$\Delta_{Z\text{-}E}$(*P-a*) − $\Delta_{Z\text{-}E}$(MF_*P-a*) (2)						
$\Delta\Delta_{ZE}V_T(A,B)$	C1	O2	O3	H4	Me5	$\Delta\Delta_{ZE}E_{net}(B)$	$\Delta\Delta_{ZE}V_T(A,B)$	C1	O2	O3	H4	Me5	H_p	$\Delta\Delta_{ZE}E_{net}(B)$
C1						22.2	C1							−34.1
O2	−39.8					−1.8	O2	57.2						−13.8
O3	37.5	1.6				−5.1	O3	93.7	−43.5					−20.6
H4	−5.8	5.1	2.6			4.5	H4	3.4	−2.3	5.2				10.5
Me5	−15.6	21.1	−55.8	−9.2		33.7	Me5	−41.0	17.4	14.8	−17.4			−15.6
							H_p	−44.1	10.1	8.7	7.7	63.4		−11.7

	$\Delta_{Z\text{-}E}$(*P-a*) − $\Delta_{Z\text{-}E}$(MF)						
$\Delta\Delta_{ZE}V_T(A,B)$	C1	O2	O3	H4	Me5	H_p	$\Delta\Delta_{ZE}E_{net}(B)$
C1							−11.9
O2	17.4						−15.6
O3	131.2	−41.9					−25.8
H4	−2.4	2.8	7.8				15.0
Me5	−56.6	38.5	−41.0	−26.5			18.0
H_p	−44.1	10.1	8.7	7.7	63.4		−11.7

	$\Delta\Delta_{ZE}E_{corr}$
MF → *P-a*	−5.2
(1)	1.6
(2)	−6.9

[a]All values are in kJ mol^{-1}.

the positive terms are those that favor the inversion of the *Z* preference. The most important ones are those associated with the interaction between C1···O3 and Me5···H_p. Considering the protonation process in two steps, every single term can be split into two contributions: one accounting for the rearrangement process and the other for the protonation itself. In this case, the anti-*Z* behavior of both interactions lies, basically, in the second step (93.7 and 63.4 kJ mol^{-1}, respectively − Table 5). As a consequence, the origin of the inversion relies directly on the presence of H_p and not on the nuclear reorganization of the HCOOMe fragment that accompanies the protonation.

Another effect of interest lies on the O2···Me5 interaction. The strength of this interaction for favoring the *Z* preference is smaller in the protonated system (−109.9 vs −148.4 kJ mol^{-1}, which results in $\Delta\Delta_{ZE}V_T$= 38.5 kJ mol^{-1} for this pair of atoms: Table 5). In other words, the protonation in the carbonyl position also weakens the interaction that was postulated as the most important one for the explanation of the *Z* preference in these kinds of systems.

When R′= H is replaced by an electron donor or acceptor group, *P-a* protonation also reverses the conformational preference, favoring the *E* arrangement (Table 6). Moreover, while this protonation changes $\Delta_{ZE}E$ values ($\Delta_{ZE}E$= E_Z − E_E) from −19.8 to 16.3 kJ mol^{-1} in MF (Table 6), resulting in increasing $\Delta_{ZE}E$ by 36.1 kJ mol^{-1}, this effect is quantitatively enlarged in all the derivatives, but R′= F.

3.4. Effect of the Other Protonations in the *Z/E* Electron Reorganization. An inversion of ΔN(Me5) and ΔN(O3) values respect to MF (Table 4) is also observed in protonation *P-b*. These inversions are smaller, in absolute values, than in *P-a*, though. The calculation of $f_{Z/E}$ (see Appendix) yields 0.64, which gives a qualitative explanation for this fact. For this protonation, the *Z*-preference is not reversed, but the conformational energy difference $|\Delta_{ZE}E|$ is half of that found for MF (Table 1). Taking the *P-a* protonation as a model, the origin of this fact could lie in the decrease of the weight/contribution of the Me5···H_p interaction to $|\Delta_{ZE}E|$.

On the other hand, *P-c* protonation is characterized by elongation of the C1−O3 distance (Table 1) and by the loss of the planarity in the OCOC moiety (Figure 8). It suggests that the system evolves to the dissociation (alcohol and HCO^+ cation). In addition, the $\Delta_{ZE}E$ value (Table 1) is still negative,

Table 6. Electronic Energies (in au) for the *Z* and *E* Arrangement of MF Derivatives, *E*(R′COOMe), and Relative energies for the Corresponding *P-a* Protonated Forms, *E*(*P-a*), and for the R′COOMe Molecule in the *P-a* Geometry, *E*(R′COOMe)$^{P\text{-}a}$, with Regard to *E*(R′COOMe)[a]

		E(R′COOMe)	*E*(R′COOMe)$^{P\text{-}a}$	*E*(*P-a*)
Z	R′ = H	−229.148 68	*37.6*	*-795.1*
Z	R′ = CF_3	−566.300 16	*45.2*	*-748.3*
Z	R′ = CH_3	−268.487 31	*40.0*	*-838.0*
Z	R′ = CN	−321.403 72	*36.9*	*-733.6*
Z	R′ = F	−328.433 89	*56.3*	*-745.9*
Z	R′ = OH	−304.420 55	*49.8*	*-805.3*
E	R′ = H	−229.141 13	*39.6*	*-831.2*
E	R′ = CF_3	−566.287 80	*43.2*	*-791.4*
E	R′ = CH_3	−268.475 28	*39.8*	*-879.6*
E	R′ = CN	−321.395 56	*36.7*	*-772.7*
E	R′ = F	−328.428 56	*57.7*	*-780.9*
E	R′ = OH	−304.415 32	*50.9*	*-844.3*
Z-E	R′ = H	*-19.8*	*-21.8*	*16.3*
Z-E	R′ = CF_3	*-32.4*	*-30.4*	*10.7*
Z-E	R′ = CH_3	*-31.6*	*-31.4*	*9.9*
Z-E	R′ = CN	*-21.4*	*-21.2*	*17.6*
Z-E	R′ = F	*-14.0*	*-15.4*	*21.1*
Z-E	R′ = OH	*-13.7*	*-14.8*	*25.2*

[a]The difference between *Z* and *E* conformers is also shown for each species. All relative energies (in *italics*) are in kJ mol^{-1}.

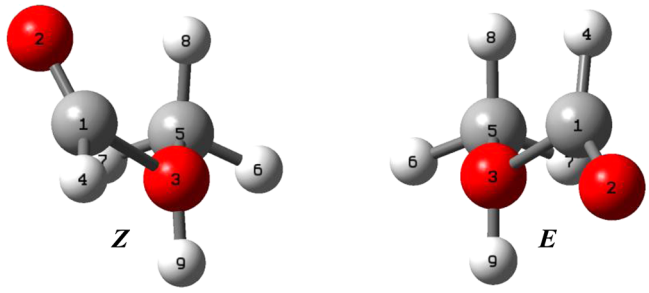

Figure 8. *Z* and *E* conformers of the *P-c* protonated form of MF (MP2 level).

dx.doi.org/10.1021/jp311472b | J. Phys. Chem. A 2013, 117, 257−265

although very small (−3.4 kJ mol^{-1} at the MP2 level), as is expected due to the similarity with the *N*-methylformamide (ΔE is −6.3 kJ mol^{-1} at the MP2 level).[6] Because of that, we consider that the computational cost of a QTAIM-based energy partitioning is not justified.

4. CONCLUSIONS

In a previous paper, a QTAIM-based energy partitioning was carried out in order to understand the origin for the **Z** preference in formic acid and related units.[6] The same analysis lets us to comprehend why the carbonyl protonation of methyl formate at the side of the methyl group shows an inversion of **Z** preference. The origin of this inversion is based in the modification of the interaction that takes place between the atoms in the ether group (due to the electron density reorganization caused by the presence of the proton in the system) and between the methyl group and the proton (whose repulsion is bigger in the **Z** arrangement).

Furthermore, the protonation in *P-a* also affects the principal interaction that gives rise to the **Z** preference in methyl formate: the interaction between the methyl group and the carbonyl oxygen, in the carbonyl protonation, is less efficient than in the neutral molecule.

The most important changes in the electron density distribution and in the energy terms that take place during the protonation are due to the introduction of the proton in the system and do not arise from the geometry reorganization.

Finally, replacing carbonyl hydrogen by diverse electron acceptor or donor substituents does not modify the main trends observed for methyl formate.

APPENDIX: DIRECTIONALITY OF THE ELECTRON DENSITY TRANSFER

Around 70% of the molecular charge (+1 au) is located in H_p basin, making it the most significant ρ-polarizing center in the molecule. Thus, any fact favoring reinforcement of electron density in H_p neighborhood should be stabilizing. Therefore, relative orientation of bond paths with regard to H_p affects the efficiency of diverse ρ-reorganizations in the molecule.

Consider the vector $\mathbf{v}_{\rho,i}$ (Scheme 2) connecting the methyl carbon to O3 at the *i* conformer and whose magnitude is the

Scheme 2

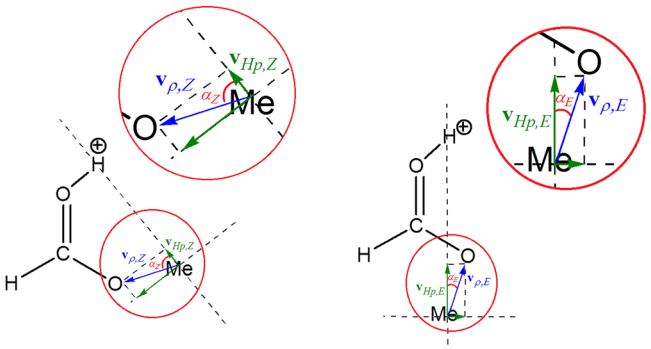

possible electron density transferred by the methyl group to O3 due to the conformational change. The projection of $\mathbf{v}_{\rho,i}$ along the H_p-Me line of junction, $\mathbf{v}_{Hp,i}$, can be considered, approximately, as a qualitative measure of how efficient is removing electron density from the methyl group in order to approach it to the proton. It is obvious that $|\mathbf{v}_{Hp,i}|=\cos\alpha_i\cdot|\mathbf{v}_{\rho,i}|$, being α_i the angle between $\mathbf{v}_{Hp,i}$ and $\mathbf{v}_{\rho,i}$.

With this in mind, the factor defined by eq 7 can be taken as the relative effectiveness of the transfer Me5→O3 toward H_p. The MP2 optimized geometries yield $f_{Z/E}$= 0.28 for *P-a* and, consequently, the transference in ***E*** is 3.5 times (1/0.28) more effective than in **Z**, according to this mechanics.

$$f_{Z/E} = \frac{|v_{Hp,Z}|/|v_{\rho,Z}|}{|v_{Hp,E}|/|v_{\rho,E}|} = \frac{\cos\alpha_Z}{\cos\alpha_E} \quad (7)$$

It is important to remark that this mechanism only gives us a qualitative explanation for the variations in $\Delta N(\Omega)$ values due to the presence of the proton H_p in the system.

AUTHOR INFORMATION

Notes

The authors declare no competing financial interest.

ACKNOWLEDGMENTS

D.F.-C. thanks the Spanish Government for an FPU fellowship. The authors also thank CESGA for free access to its computational facilities, "Xunta de Galicia" for funding this research through project INCITE08PXIB314224PR, and Dr. Nicolás Otero for his useful comments on this paper.

REFERENCES

(1) Juaristi, E.; Cuevas, G. *The Anomeric Effect*; CRC Press: Boca Raton, FL, 1995.
(2) Nelson, D. L.; Cox, M. M. *Lehninger Principles of Biochemistry*; W.H. Freeman and Company: New York, 2005.
(3) Mo, Y. *Nat. Chem* **2010**, *2*, 666−671.
(4) Bader, R. F. W. *Atoms in Molecules, A Quantum Theory*; International Series of Monographs in Chemistry 22;Oxford University Press: Oxford, U.K., 1990.
(5) Bader, R. F. W. *Chem. Rev.* **1991**, *91*, 893−928.
(6) Ferro-Costas, D.; Otero, N.; Graña, A. M.; Mosquera, R. A. *J. Comput. Chem.* **2012**, *33*, 2533−2543.
(7) Frisch, M. J.; Trucks, G. W.; Schlegel, H. B.; Scuseria, G. E.; Robb, M. A.; Cheeseman, J. R.; Montgomery, Jr., J. A.; Vreven, T.; Kudin, K. N.; Burant, J. C.; et al. *Gaussian 03*, Revision E.01, Gaussian, Inc.: Wallingford CT, 2004.
(8) Biegler-König, F. W.; Bader, R. F. W.; Tang, T.-H. *J. Comput. Chem.* **1982**, *13*, 317−328.
(9) Rousseau, B.; Peeters, A.; Van Alsenoy, C. *Chem. Phys. Lett.* **2000**, *324*, 189−194.
(10) Blanco, M. A.; Martín Pendás, A.; Francisco, E. *J. Chem. Theory Comput.* **2005**, *1*, 1096−1109.
(11) Vila, A.; Mosquera, R. A. *J. Phys. Chem. A* **2000**, *104*, 12006−12013.
(12) Vila, A.; Mosquera, R. A. *Tetrahedron* **2001**, *57*, 9415−9422.
(13) Mandado, M.; Van Alsenoy, C.; Mosquera, R. A. *J. Phys. Chem. A* **2004**, *108*, 7050−7055.
(14) González Moa, M. J.; Mosquera, R. A. *J. Phys. Chem. A* **2005**, *109*, 3682−3686.
(15) González Moa, M. J.; Mandado, M.; Mosquera, R. A. *Chem. Phys. Lett.* **2006**, *428*, 255−261.
(16) González Moa, M. J.; Mosquera, R. A. *J. Phys. Chem. A* **2003**, *107*, 5361−5367.
(17) Estévez, L.; Mosquera, R. A. *Chem. Phys. Lett.* **2008**, *451*, 121−126.
(18) Mandado, M.; Van Alsenoy, C.; Mosquera, R. A. *J. Phys. Chem. A* **2005**, *109*, 8624−8631.
(19) Bader, R. F. W.; Chang, C. *J. Phys. Chem.* **1989**, *93*, 2946−2956.
(20) González Moa, M. J.; Mosquera, R. A. *J. Phys. Chem. A* **2006**, *110*, 5934−5941.

(21) Otero, N.; Mandado, M.; Mosquera, R. A. *J. Phys. Chem. A* **2007**, *111*, 5557−5562.